TANG FRAGMENT OF A KNIFE HR-6567 - LEADED BRONZE - LATE BRONZE AGE - SWITZERLAND

Artefact name Tang fragment of a knife HR-6567

Authors Marianne. Senn (Empa, Dübendorf, Zurich, Switzerland) & Christian. Degrigny (HE-Arc CR, Neuchâtel, Neuchâtel, Switzerland) & Naima. Gutknecht (HE-Arc CR, Neuchâtel, Neuchâtel, Switzerland) & Rémy. Léopold (HE-Arc CR, Neuchâtel, Neuchâtel, Switzerland)

Url /artefacts/1039/

The object

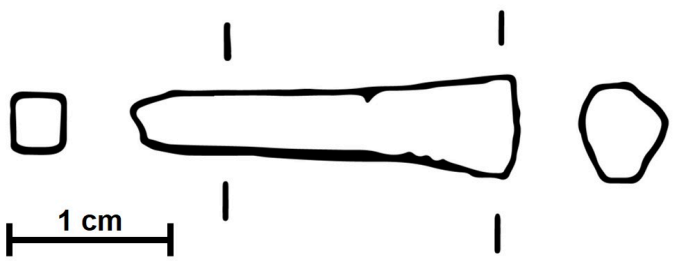


Fig. 1: Tang fragment of a knife (after Rychner-Faraggi 1983, plate 35.26),

Credit Laténium.



Fig. 2: Dense and brown-yellow corrosion product (detail) of the tang fragment of a knife,

Credit HE-Arc CR, N.Gutknecht/L.Rémy.

This work is licensed under CC BY-NC-ND 4.0

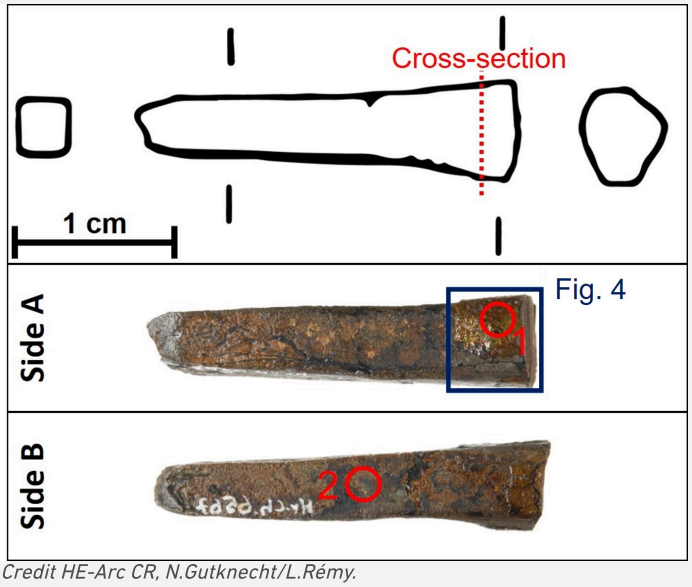
Description and visual observation

Description of the artefact	Tang fragment with shiny brown-yellow corrosion products still in place locally (Fig. 2). Dimensions: L = 2.9cm; Ømax. = 6.8mm; WT = 4.9g.
Type of artefact	Household implement
Origin	Hauterive - Champréveyres, Neuchâtel, Neuchâtel, Switzerland
Recovering date	Excavation in 1983-1985, layer 3
Chronology category	Late Bronze Age
chronology tpq	1054 B.C.
chronology taq	1000 B.C.
Chronology comment	Hallstatt B1 (1054/1037BC _ 1000BC)
Burial conditions / environment	Lake
Artefact location	Laténium, Neuchâtel, Neuchâtel
Owner	Laténium, Neuchâtel, Neuchâtel
Inv. number	HR 6567
Recorded conservation data	No conservation data available, but a coating and inventory number is visible on the surface.

Complementary information

The object was sampled in 1987 for analysis. Documentation of the strata in binocular mode on the remaining fragment of the object was performed in 2022.

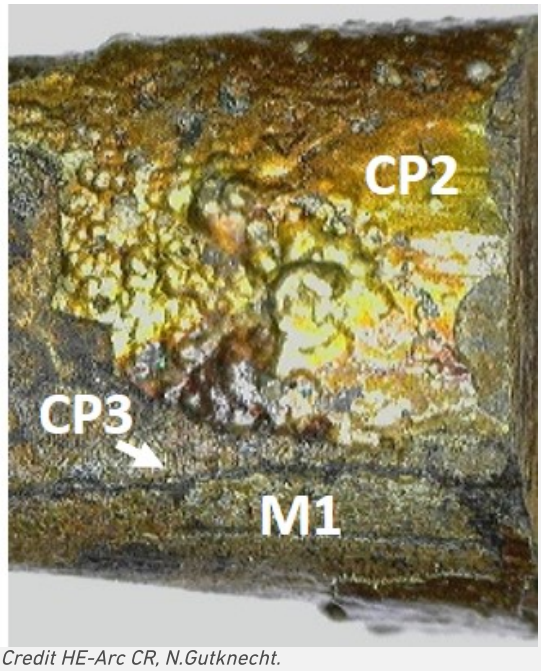
Study area(s)



Credit HE-Arc CR, N.Gutknecht/L.Rémy.

Fig. 3: Location of cross-section on drawing before sampling and both sides of fragment (after sampling) with location of the detail of Fig. 4 and XRF analysis areas (red circles),

This work is licensed under CC BY-NC-ND 4.0



Credit HE-Arc CR, N.Gutknecht.

Fig. 4: Corrosion structure (detail) from Fig. 3 showing some of the documented strata in Fig. 5,

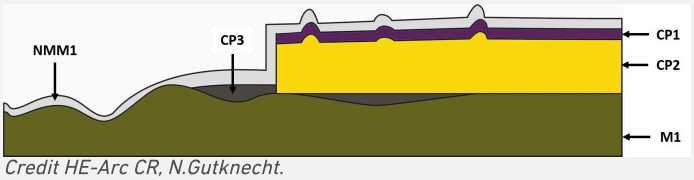
Binocular observation and representation of the corrosion structure

The schematic representation below gives an overview of the corrosion structure encountered on the fragment from a first visual macroscopic observation.

Strata	Type of stratum	Principal characteristics
NMM1	Non-metalic material	Film/coating, transparent, thin, continuous
CP1	Corrosion product	Brown, pearly, thin, discontinuous, compact
CP2	Corrosion product	Dark yellow, thick, discontinuous, compact, hard
CP3	Corrosion product	Layer, dark grey, thin, scattered, non-compact, soft
M1	Metal	Olive, thick, metallic, soft

Table 1: Description of the principal characteristics of the strata as observed under binocular and described according to Bertholon's method.

The NMM1 seems to be a polymer coating added after excavation of the object.



Credit HE-Arc CR, N.Gutknecht.

Fig. 5: Stratigraphic representation of the corrosion structure of the tang of knife by macroscopic and binocular observation with reference to Fig. 4,

MiCorr stratigraphy(ies) – Bi

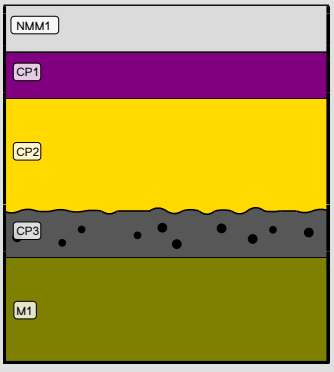


Fig. 6: Stratigraphic representation of the corrosion structure of the tang of a knife observed macroscopically under binocular microscope using the MiCorr application with reference to the whole Fig. 5. The characteristics of the strata, such as discontinuity, are accessible by clicking on the drawing that redirects you to the search tool by stratigraphy representation, Credit HE-Arc CR, N.Gutknecht.

This work is licensed under CC BY-NC-ND 4.0

Sample(s)

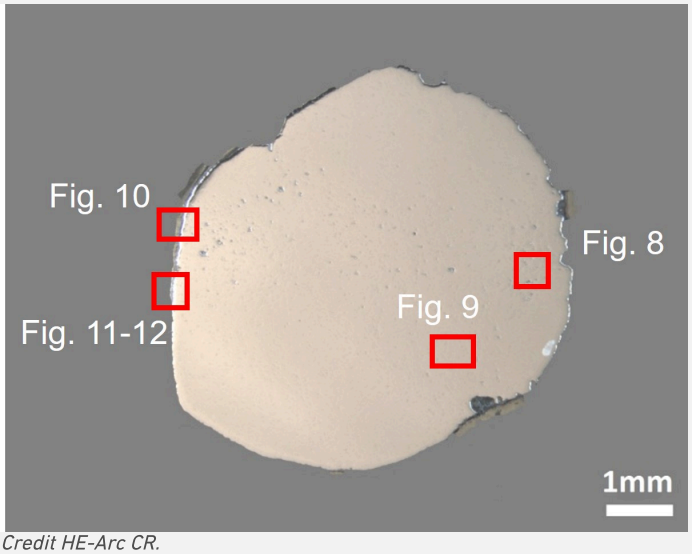


Fig. 7: Micrograph of the cross-section of the sample taken from the tang fragment of a knife showing the location of Figs. 8 to 12,

Credit HE-Arc CR.

Description of sample	This cross-section shows a lateral cut through the tang (Fig. 3). Most of the corrosion structure is absent (Fig. 7).
Alloy	Leaded Bronze
Technology	Cold worked with partial annealing
Lab number of sample	MAH 87-196
Sample location	Musées d'art et d'histoire, Genève, Geneva
Responsible institution	Musées d'art et d'histoire, Genève, Geneva
Date and aim of sampling	1987, metallography and corrosion characterisation

Complementary information

None.

Analyses and results

Analyses performed:

Non-invasive approach

XRF with handheld portable X-ray fluorescence spectrometer (NITON XL5). General Metal mode, acquisition time 60s (filters: Li20/Lo20/M20).

Invasive approach (on the sample)

Metallography (etched with ferric chloride reagent), Vickers hardness testing, ICP-OES, SEM/EDS (conditions provided in the About tab of the MiCorr application), XRD.

Non invasive analysis

XRF analyses of the tang fragment of a knife were carried out on two representative areas (Fig. 3). Point 1 was done on the dark yellow corrosion layer (CP2), while point 2 was performed on the remaining metal surface. For both points, soil, corrosion products and metal are analyzed at the same time.

The metal is presumably a tin bronze alloy. The other elements detected are: Fe, S, Pb, Si, Al, Sb, As, Co, Ag, Zn.

Results of point 1 are very different from those of point 2, they indicate the enrichment in Fe and in S and depletion in Cu.

Elements (mass %)	Cu		Fe		S		Sn		Pb		Si		Al		Sb		As		Co		Ag		Zn		
	%	+\-2σ	%	+\-2σ	%	+\-2σ	%	+\-2σ	%	+\-2σ	%	+\-2σ	%	+\-2σ	%	+\-2σ	%	+\-2σ	%	+\-2σ	%	+\-2σ	%	+\-2σ	Total

This work is licensed under CC BY-NC-ND 4.0

1	37.0	0.1	32.0	0.09	23.5	0.08	4.0	0.02	<0.1	0.01	1.5	0.06	0.5	0.1	0.4	0.01	0.2	0.01	0.2	0.04	0.1	0.01	<0.1	0.02	99.4
2	77.0	0.1	1.0	0.02	3.5	0.03	9.0	0.04	2.0	0.03	2.0	0.05	0.5	0.1	0.7	0.02	2.0	0.04	0.2	0.01	0.3	0.01	<0.1	0.02	99.5

Table 2: Chemical composition of the surface of the tang at two representative areas shown in Fig. 3. Method of analysis: XRF.

Metal

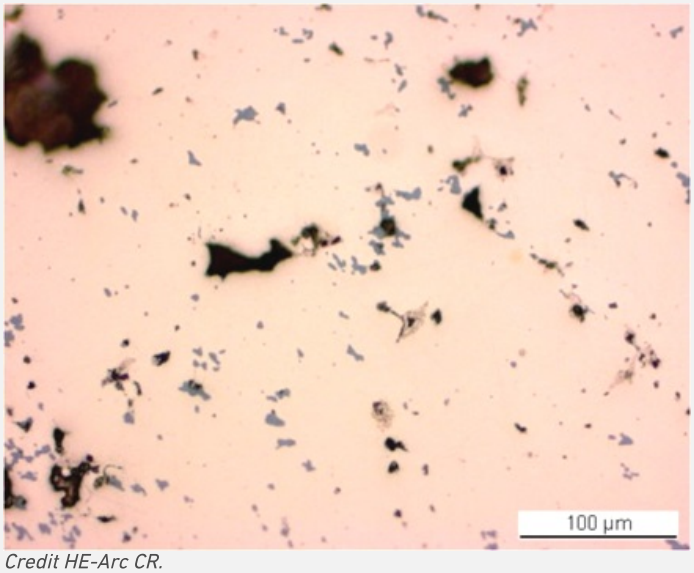
The remaining metal is a leaded bronze (Table 2) containing numerous copper sulphide and tiny Pb inclusions (Figs. 8-10, 12 and Table 4). The porosity within the metal is high, particularly along a band through the middle of the sample (Figs. 7 and 8). The etched structure of the leaded bronze shows small, regular polygonal grains, some with twinning (Fig. 9). Slip lines appear in grains close to the metal surface (Fig. 9). The average hardness of the metal is HV1 120.

Elements	Cu	Sn	Pb	Ni	Sb	As	Co	Ag	Fe	Zn
mass%	87.52	8.02	1.46	1.04	0.81	0.60	0.24	0.21	0.05	0.03

Table 3: Chemical composition of the metal. Method of analysis: ICP-OES, Laboratory of Analytical Chemistry, Empa.

Elements	O	S	Fe	Cu	Total
mass%	1.5	20	1.0	71	**93**

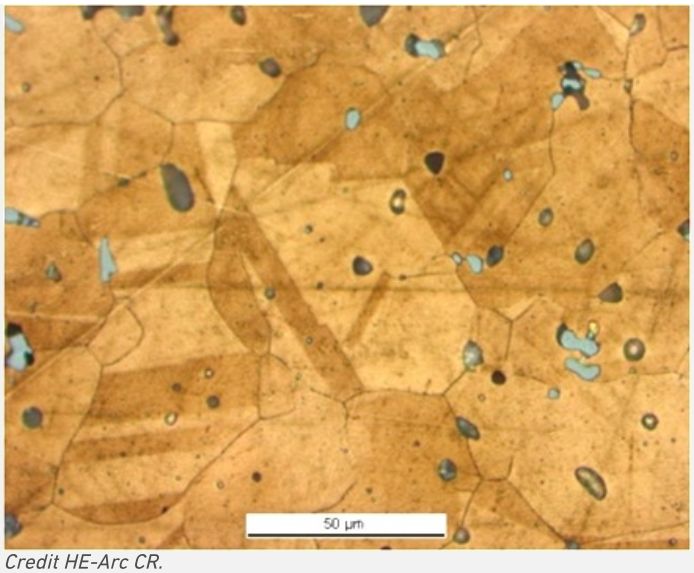
Table 4: Chemical composition of dark-grey inclusions. Method of analysis: SEM/EDS, Laboratory of Analytical Chemistry, Empa.



Credit HE-Arc CR.

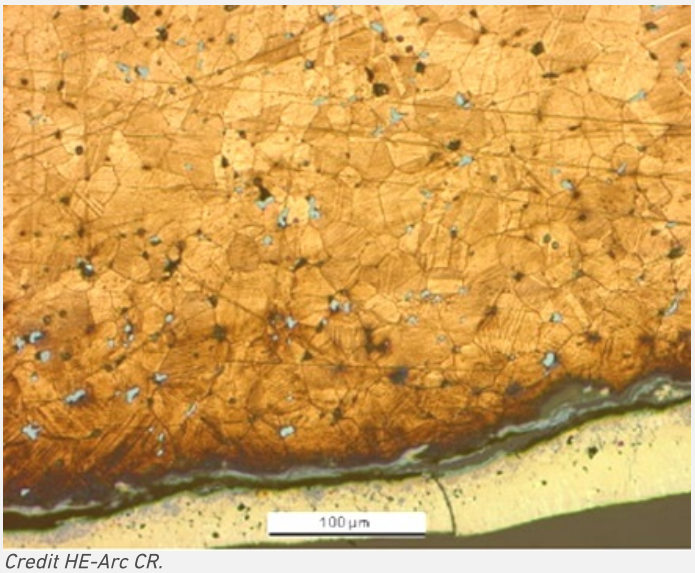
Fig. 8: Micrograph of the metal sample from Fig. 7 (detail), unetched, bright field. In pink the metal, in black the porosity and in dark-grey copper sulphide inclusions,

This work is licensed under CC BY-NC-ND 4.0



Credit HE-Arc CR.

Fig. 9: Micrograph of the metal sample from Fig. 7 (detail), etched, bright field. Angular and twinned grains are revealed as well as copper sulphide inclusions in grey,



Credit HE-Arc CR.

Fig. 10: Micrograph of the metal sample from Fig. 7, etched, bright field (rotated by 270°, detail). Angular grains with slip lines can be seen as well as copper sulphide inclusions in grey,

Microstructure	Polygonal and twinned grains + strain lines (metal surface) with pores
First metal element	Cu
Other metal elements	Co, Ni, As, Ag, Sn, Sb, Pb

Complementary information

None.

Corrosion layers

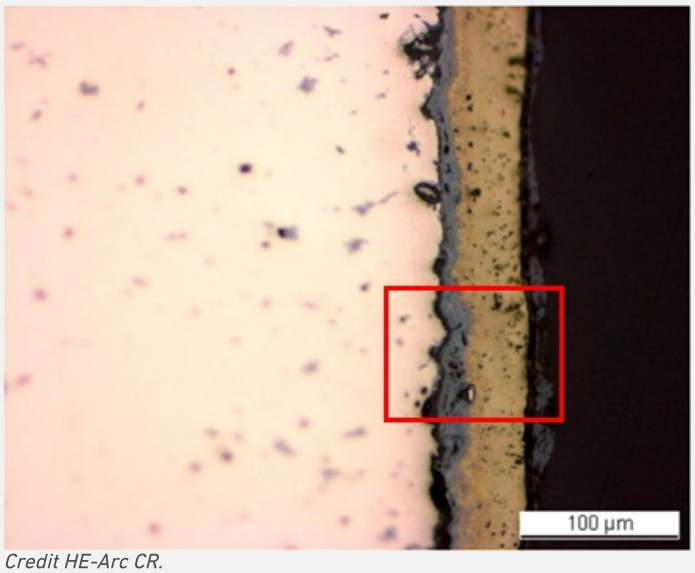
The metal has lost most of its original corrosion layer, the remainder having an average thickness between 60 and 190µm (Fig. 6). In some areas up to three corrosion strata are visible (Fig. 11). In polarised light (Fig. 12), the corrosion stratigraphy appears more clearly: it is composed of a dense black inner layer, an intermediate thick brown layer with bright spots (indicating porosity) and an outer red layer with white particles. The elemental chemical distribution of the SEM image reveals that the black inner layer (CP3) is Sn-rich, but contains Cu, O, Fe, Si, P, Pb, Ni, As, Ca and S (Table 5, Figs. 12-13). The brown layer (CP2) contains S, Fe and Cu and has a composition similar to chalcopyrite/$CuFeS_2$ (Table 5, Figs. 12-13). This was confirmed by past XRD analyses carried out by Schweizer (1994, museum report (1987)). The red layer (CP1) is an iron oxide (main elements Fe and O) and is contaminated with calcite/$CaCO_3$ particles (S1) (Table 5, Figs. 12-13).

Elements	O	Fe	Ni	Cu	Si	P	S	Ca	As	Sn	Pb	Total
CP1, red layer	37	51	1.8	<	<	<	<	1.5	0.8	<	<	**93**
CP2, brown layer	<	30	<	42	<	<	35	<	<	<	<	**107**

This work is licensed under CC BY-NC-ND 4.0

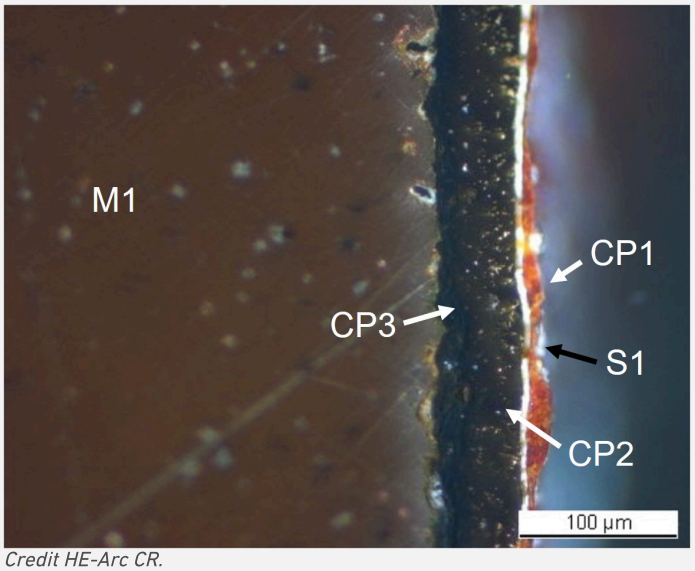
CP2, white particles	50	<	<	0.6	<	<	<	39	<	<	<	**90**
CP3, black layer	39	4.8	1.2	5.2	3.9	3.7	<	<	0.7	37	3.7	**100**

Table 5: Chemical composition (mass %) of the corrosion layers (from Figs. 12). Method of analysis: SEM/EDS, Laboratory of Analytical Chemistry, Empa.



Credit HE-Arc CR.

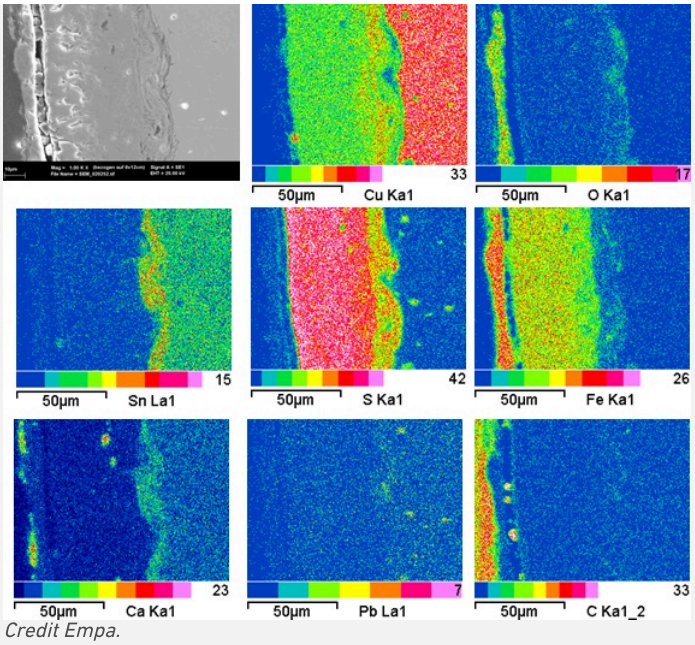
Fig. 11: Micrograph of the metal sample from Fig. 7 (reversed picture, detail), unetched, bright field. From left to right: metal (in pink), inner light-grey layer, intermediate brown layer and top dark-grey layer. The area selected for elemental chemical distribution (Fig. 13) is marked by a red rectangle,



Credit HE-Arc CR.

Fig. 12: Micrograph of the same area as Fig. 11 and corresponding to the stratigraphy of Fig. 14, polarized light. From left to right: metal (in brown) covered with a corrosion layer consisting of a black layer, an intermediate brown layer with bright spots, a crack (white line) and a red layer with white particles,

This work is licensed under CC BY-NC-ND 4.0



Credit Empa.

Fig. 13: SEM image, SE-mode, and elemental chemical distribution of the selected area of Fig. 11 (reversed picture). Method of examination: SEM/EDS, Laboratory of Analytical Chemistry, Empa,

Corrosion form	Uniform
Corrosion type	lake patina (Schweizer 1994)

Complementary information

None.

MiCorr stratigraphy(ies) – CS

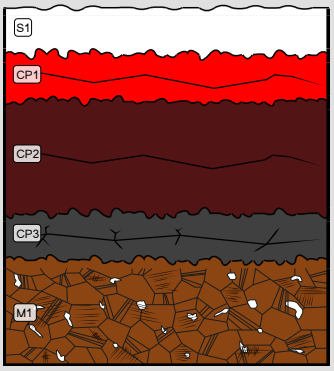


Fig. 14: Stratigraphic representation of the sample taken from the tang fragment of a knife in cross-section (dark field) using the MiCorr application. The characteristics of the strata are accessible by clicking on the drawing that redirects you to the search tool by stratigraphy representation. This representation can be compared to Fig. 12, Credit HE-Arc CR.

Synthesis of the binocular / cross-section examination of the corrosion structure

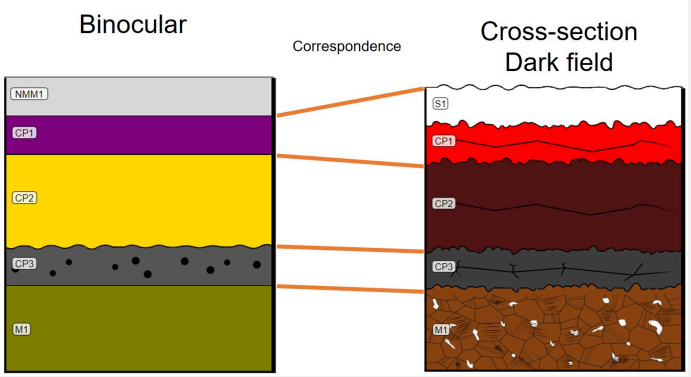
NMM1 in binocular mode is not observed in cross-section mode, as the cross-section does not show any coating.

CP1 in binocular mode is documented as sediment (S1) and CP1 in cross-section mode. But it is not clear if it matches the CP1 from cross-section, which is a Fe-rich layer, or if CP1 from binocular mode developed as an atmospheric corrosion after the excavation and is therefore not present on the embedded sample.

CP2 and CP3 in binocular mode match CP2 and CP3 in cross-section mode.

On cross-section, it was possible to describe and analyze the microstructure of the metal.

This work is licensed under CC BY-NC-ND 4.0



Credit HE-Arc CR, N.Gutknecht/L.Rémy

Fig. 15: Stratigraphic representation side by side of binocular view and cross-section (dark field),

Conclusion

The tang fragment is made from a leaded bronze and has been cold worked on the top surface after annealing. The SEM/EDS examination and past XRD analyses indicate the presence of chalcopyrite in the corrosion layer, typical of lake context (Schweizer 1994). This corrosion layer is enriched with Sn close to the metal surface and depleted of Cu on the outer surface. The limit of the original surface most probably lies between the Sn-rich inner layer and the Fe and S-rich outer layers. The presence of iron oxides on top of the copper corrosion layer has not yet been explained. The corrosion is a type 1 according Robbiola et al. 1998.

This object was first sampled in 1987. Thanks to an extensive documentation on cross-section and comparison with similar objects (see references), Schweizer defines a "lake patina" typology on this object that gives information about the burial's environment. In fact, according to his research, the dense "lake patina", analyzed as chalcopyrite, can only be generated in the presence of sulfate-reducing bacteria. Conditions for those bacteria are an anaerobic, humid, and S and Fe-rich environment. This object was probably abandoned directly into the lake

References

References on object and sample

Object files in MiCorr

1. MiCorr_Pin or needle fragment HR-3031
2. MiCorr_Tang fragment of a knife HR-6246
3. MiCorr_Pin HR-18152
4. MiCorr_Pin HR-17773
5. MiCorr_Pin HR-3071
6. MiCorr_Pin HR-18603
7. MiCorr_Pin HR-3389

References object

8. Rychner-Faraggi A-M. (1993) Hauterive – Champréveyres 9. Métal et parure au Bronze final. Archéologie neuchâteloise, 17 (Neuchâtel).
9. Hochuli, S. et al. (1988) SPM III Bronzezeit , Verlag Schweizerische Gesellschaft für Ur- und Frühgschichte Basel, 76-77, 379.

References sample

10. Empa Report 137 695/1991, P.O. Boll.
11. Rapport d'examen, Lab. Musées d'Art et d'Histoire, Geneva GE, 87-194 à 87-197.
12. Schweizer, F. (1994) Bronze objects from Lake sites: from patina to bibliography. In: Ancient and historic metals, conservation and scientific research (eds. Scott, D.A., Podany, J. and Considine B.B.), The Getty Conservation Institute, 33-50.

References on analytic methods and interpretation

13. Robbiola, L., Blengino, J-M., Fiaud, C. (1998) Morphology and mechanisms of formation of natural patinas on archaeological Cu-Sn alloys, Corrosion Science, 40, 12, 2083-2111.

This work is licensed under CC BY-NC-ND 4.0